Input Current Ripple Analysis of Nine-Phase PWM Inverters

Dadan Nurafiat[1] and Pekik Argo Dahono[2]

School of Electrical Engineering and Informatics, Institute of Technology Bandung

Jl. Ganesa 10, Bandung 40132, Indonesia

[1]dadan@konversi.ee.itb.ac.id

[2]pekik@konversi.ee.itb.ac.id

Abstract— **An input current-ripple analysis of nine-phase pulse width modulated (PWM) inverter is presented in this paper. The current-ripple is analyzed using a frequency domain approach. Two configurations of nine-phase inverter (symmetrical and asymmetrical) are analyzed. Analysis results show that symmetrical configuration has lower input current-ripple compared to asymmetrical configuration. Several experimental results are included to show the validity of the proposed analysis method.**

Keywords— Input ripple, multiphase, PWM.

I. INTRODUCTION

Recent developments in power electronics have led the wide applications of multiphase systems. Multiphase drives have advantages over conventional three-phase drives such as reduction in the phase current of inverter, better reliability, and higher power density [1]-[5]. A lot of works on PWM techniques for multiphase inverters were also published [6]-[9].

Information about input current ripple of an inverter is important for DC filter specification. A lot of works on input current ripple analysis were published [10]-[13]. Time domain and frequency domain analysis methods have been proposed but most of them are concentrated on three-phase PWM inverters. Just a few of them are dealing with multiphase PWM inverters [14]-[15].

McGrath and Holmes [16] have proposed an analysis of dc-link current using a frequency domain approach. In their work, the spectrum of dc-link current harmonics under various PWM techniques is investigated. How to determine the rms value of the input current ripple, however, has not been shown. Moreover, their work is still limited to three-phase PWM inverters.

This paper presents an input current ripple analysis of nine-phase carrier-based PWM inverter. The analytical expressions for the ripple component of input current are derived. Based on these expressions, it is shown that the rms value of input current ripple of nine-phase PWM inverter is influenced by the value of output current, modulation index, and load power factor. The inverter input current ripple cannot be reduced by increasing the switching frequency. Symmetrical and asymmetrical nine-phase configurations are compared. Several experimental results are included to show the validity of the proposed analysis method.

II. NINE-PHASE PWM INVERTER

Fig 1 shows the scheme of nine-phase inverter which is used in this investigation. It is assumed that the dc voltage source E_d is constant and ripple free. In the proposed analysis method, the output currents are assumed to be balanced and sinusoidal. Though various PWM techniques have been developed, the most commonly used PWM technique for this application is carrier-based PWM technique. It employs a comparison between a reference signal and a high-frequency triangular carrier signal. The result of comparison determines the ON-OFF signals for inverter switching devices. The reference signals are usually pure sinusoidal signals. Sinusoidal signals are used here because as it was shown in [11] and [15], third harmonic signal injections cannot be used to reduce the inverter input current ripple. In the analysis, it is also assumed that inverter switching devices are ideal switches.

There are various possible stator winding connections to create a nine-phase AC motor. The most common connections are triple three-phase stator connections. In this case, nine phase system is created by using three three-phase stator windings. Each three-phase stator winding is usually connected in wye connection. Among three three-phase stator windings are displaced by either 20 (asymmetrical) or 40 (symmetrical) electrical degrees. The three neutral points are isolated. See Fig. 2. By using these displacement angles, the torque ripple and input current ripple under square wave inverter operation will be reduced significantly.

The output currents of inverter are assumed to be balanced and sinusoidal. The output currents of inverter can be written as follows:

$$i_x = \sqrt{2} I_l \sin\left[\theta - \phi - \theta_{ox}\right] \quad (1)$$

where I_l is rms value of the load currents, ϕ is load power factor angle, $\theta=\omega_o t$ with ω_o is the fundamental angular

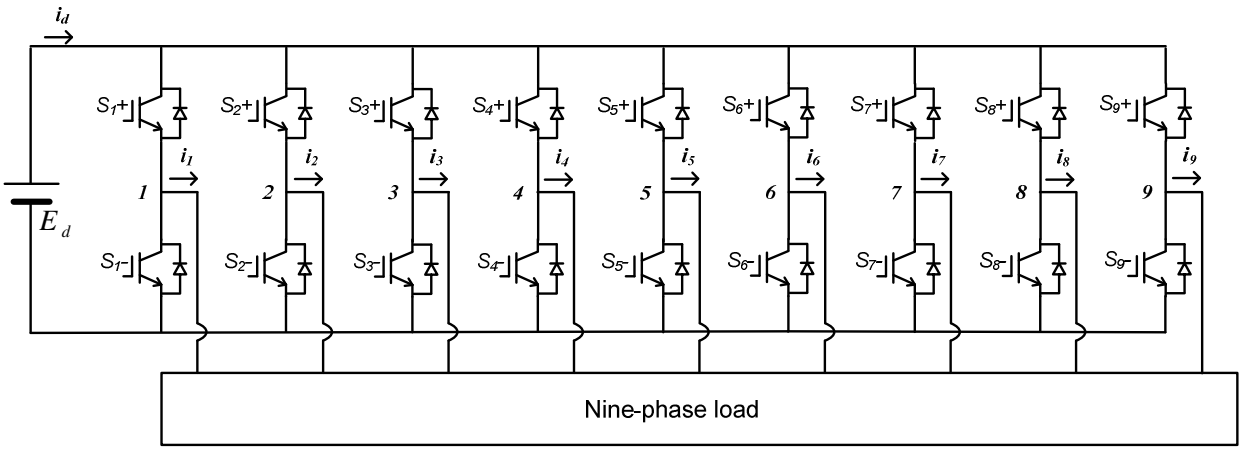

Fig. 1. Nine-phase inverter.

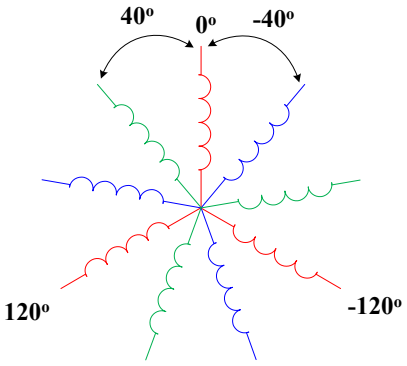

(a) Symmetrical.

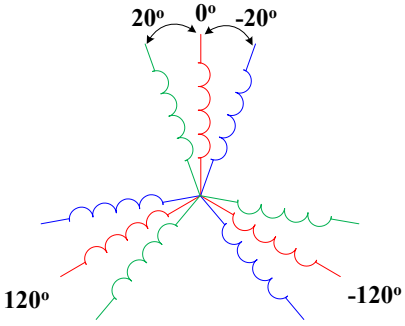

(b) Asymmetrical.

Fig. 2. Nine-phase configurations.

frequency of the inverter, and θ_{ox} is the fundamental phase angle.

For symmetrical configuration, the fundamental phase angle are as follows :

$$\theta_{ox} = (x-1)\frac{2\pi}{9} \tag{2}$$

for $x = 1, 2, 3, \ldots, 9$.

For asymmetrical configuration, the fundamental phase angle are as follows:

$$\theta_{ox} = (x-1)\frac{\pi}{9} \tag{3}$$

for $x = 1, 2, 3$

$$\theta_{ox} = (x-4)\frac{\pi}{9} \tag{4}$$

for $x = 4, 5, 6$

$$\theta_{0x} = (x-7)\frac{\pi}{9} \tag{5}$$

for $x = 7, 8, 9$.

Input current ripple analysis of nine-phase PWM inverters will be described in the next section.

III. Analysis of Input Current-Ripple

The inverter input current can be expressed as a function of switching states and output currents as follows:

$$i_d = S_1 i_1 + S_2 i_2 + S_3 i_3 + S_4 i_4 + S_5 i_5 + S_6 i_6 + S_7 i_7 + S_8 i_8 + S_9 i_9 \tag{6}$$

where S_x is the switching states of phase x of inverter. The switching state is unity (zero) when the upper (lower) switching device of phase x is receiving an ON signal. The approach to determine the input current ripple as shown in (5) is identical to the method in [15]. In this paper, the number of phase is extended to nine phase.

The multiplication in the time domain is equivalent to convolution operation in the frequency domain [16]. In the frequency domain the input current expression is as follows:

$$\begin{aligned} i_d(\omega) = {} & S_1(\omega) i_1(\omega) + S_2(\omega) i_2(\omega) + S_3(\omega) i_3(\omega) \\ & + S_4(\omega) i_4(\omega) + S_5(\omega) i_5(\omega) + S_6(\omega) i_6(\omega) \\ & + S_7(\omega) i_7(\omega) + S_8(\omega) i_8(\omega) + S_9(\omega) i_9(\omega) \end{aligned} \tag{7}$$

From [16], the expression of switching waveform of carrier-based PWM inverter is as follows:

$$S_x(t)=\frac{1}{2}+\frac{k}{2}\cos\left(\omega_o t-\theta_{ox}\right)+\sum_{m=1}^{\infty}\sum_{n=-\infty}^{\infty}\left[\begin{array}{l}\frac{2}{m\pi}\sin\left(\left[m+n\right]\frac{\pi}{2}\right)J_n\left(m\frac{\pi}{2}k\right)\\ \times\cos\left(m\left[\omega_c t-\theta_{cy}\right]+n\left[\omega_o t-\theta_{ox}\right]\right)\end{array}\right] \quad (8)$$

where k is modulation index, m is carrier index variable, n is baseband index variable, $J_n(\xi)$ denotes a Bessel function of the first kind, with order n and argument ξ. θ_{cy} is carrier phase angle, which has zero value for single carrier utilization. θ_{ox} are obtained from (2) for symmetrical configuration or from (3)-(5) for asymmetrical configuration.

The input current expression for nine-phase PWM inverter is obtained as follows:

1. Substitute equation (2) or (3)-(5) to (1) to obtain output current for symmetrical configuration or asymmetrical configuration.
2. Transform the current equations obtained from point 1 and the respective switching functions from equation (8) to the frequency domain.
3. Substitute the result from point 2 to equation (7).
4. Transforming back the calculation result obtained from equation (7) to the time domain.

The expression of input current obtained will consist of dc value and ac value as shown in Table I. If the dc value is subtracted from the input current expression then the input current-ripple expression is obtained. The rms value of input current-ripple can be derived as follow:

$$\tilde{I}_d=\sqrt{\frac{1}{T}\int_0^T i_d^2 dt-I_{dc}^2} \quad (9)$$

where

$$I_{dc}=\frac{9\sqrt{2}}{4}kI_l\cos\phi \quad (10)$$

and T is the fundamental period of the inverter output current. Substituting expressions in Table 1 and (10) into (9) then the rms value of input current ripple can be obtained. The results are shown in Table II. The results show that the rms value of input current ripple is not influenced by the switching frequency. Thus, input current ripple cannot be reduced by increasing the switching frequency. The input current ripple is influenced by the load power factor. This result is the same as in the case of three-phase inverter. Fig. 3 shows the rms value of input current ripple as a function of modulation index for two values of load power factor. The results show that symmetrical configuration results in less ripple than asymmetrical configuration.

TABLE I
INPUT CURRENT EXPRESSIONS

Symmetrical configuration
$i_d(t)=\frac{9k}{4}\sqrt{2}I_l\cos\phi+\sum_{m=1}^{\infty}\sum_{n=-\infty}^{\infty}\left[\begin{array}{l}\left(\begin{array}{l}\frac{\sqrt{2}I_l}{m\pi}\cos\left(\left[m+n\right]\frac{\pi}{2}\right)\left[1+2\cos\left(n\frac{2\pi}{3}\right)\right]\left[1+2\cos\left(n\frac{2\pi}{9}\right)\right]\cos\phi\\ \times\left[J_{n+1}\left(m\frac{\pi}{2}k\right)-J_{n-1}\left(m\frac{\pi}{2}k\right)\right]\end{array}\right)\cos\left(m\omega_c t+n\omega_o t\right)\\ -\left(\begin{array}{l}\frac{\sqrt{2}I_l}{m\pi}\cos\left(\left[m+n\right]\frac{\pi}{2}\right)\left[1+2\cos\left(n\frac{2\pi}{3}\right)\right]\left[1+2\cos\left(n\frac{2\pi}{9}\right)\right]\sin\phi\\ \times\left[J_{n+1}\left(m\frac{\pi}{2}k\right)+J_{n-1}\left(m\frac{\pi}{2}M\right)\right]\end{array}\right)\sin\left(m\omega_c t+n\omega_o t\right)\end{array}\right]$
Asymmetrical configurarion
$i_d(t)=\frac{9k}{4}\sqrt{2}I_l\cos\phi+\sum_{m=1}^{\infty}\sum_{n=-\infty}^{\infty}\left[\begin{array}{l}\left(\begin{array}{l}\frac{I_l}{m\pi}\cos\left(\left[m+n\right]\frac{\pi}{2}\right)\left[1+2\cos\left(n\frac{2\pi}{3}\right)\right]\left[1+2\cos\left(n\frac{\pi}{9}\right)\right]\cos\phi\\ \times\left[J_{n+1}\left(m\frac{\pi}{2}k\right)-J_{n-1}\left(m\frac{\pi}{2}k\right)\right]\end{array}\right)\cos\left(m\omega_c t+n\omega_o t\right)\\ -\left(\begin{array}{l}\frac{I_l}{m\pi}\cos\left(\left[m+n\right]\frac{\pi}{2}\right)\left[1+2\cos\left(n\frac{2\pi}{3}\right)\right]\left[1+2\cos\left(n\frac{\pi}{9}\right)\right]\sin\phi\\ \times\left[J_{n+1}\left(m\frac{\pi}{2}k\right)+J_{n-1}\left(m\frac{\pi}{2}k\right)\right]\end{array}\right)\sin\left(m\omega_c t+n\omega_o t\right)\end{array}\right]$

TABLE II
RMS INPUT CURRENT RIPPLE

Symmetrical configuration
$\tilde{I}_d = \left(\sum_{m=1}^{\infty} \sum_{n=-\infty}^{\infty} \left[\left(\frac{I_l}{m\pi} \cos\left([m+n]\frac{\pi}{2} \right) \left[1+2\cos\left(n\frac{2\pi}{3} \right) \right] \left[1+2\cos\left(n\frac{2\pi}{9} \right) \right] \cos\phi \left[J_{n+1}\left(m\frac{\pi}{2}k \right) - J_{n-1}\left(m\frac{\pi}{2}k \right) \right] \right)^2 + \left(\frac{I_l}{m\pi} \cos\left([m+n]\frac{\pi}{2} \right) \left[1+2\cos\left(n\frac{2\pi}{3} \right) \right] \left[1+2\cos\left(n\frac{2\pi}{9} \right) \right] \sin\phi \left[J_{n+1}\left(m\frac{\pi}{2}k \right) + J_{n-1}\left(m\frac{\pi}{2}M \right) \right] \right)^2 \right] \right)^{\frac{1}{2}}$
Asymmetrical configurarion
$\tilde{I}_d = \left(\sum_{m=1}^{\infty} \sum_{n=-\infty}^{\infty} \left[\left(\frac{I_l}{m\pi} \cos\left([m+n]\frac{\pi}{2} \right) \left[1+2\cos\left(n\frac{2\pi}{3} \right) \right] \left[1+2\cos\left(n\frac{\pi}{9} \right) \right] \cos\phi \left[J_{n+1}\left(m\frac{\pi}{2}k \right) - J_{n-1}\left(m\frac{\pi}{2}k \right) \right] \right)^2 + \left(\frac{I_l}{m\pi} \cos\left([m+n]\frac{\pi}{2} \right) \left[1+2\cos\left(n\frac{2\pi}{3} \right) \right] \left[1+2\cos\left(n\frac{\pi}{9} \right) \right] \sin\phi \left[J_{n+1}\left(m\frac{\pi}{2}k \right) + J_{n-1}\left(m\frac{\pi}{2}k \right) \right] \right)^2 \right] \right)^{\frac{1}{2}}$

IV. EXPERIMENTAL RESULTS

A small experimental system has been constructed to verify the proposed analysis method. The scheme of the experimental system is the same as the one shown in Fig. 1. The nine-phase motors that used in this investigation are shown in Fig. 4. These motors are modification results of the existing 7.5 hp 4-pole three-phase motors. The stator windings are rewound to be symmetrical and asymmetrical nine-phase stator windings with separate neutral points. The inverter switching devices are implemented by using power MOSFETs. The carrier based PWM technique is implemented by using FPGA ALTERA DE2-70. A carrier frequency of 1000 Hz was used in this experiment. Sinusoidal reference signals were used in all experiments. To avoid a short circuit through upper-arm and lower arm switching devices of the inverter, a 3 μs dead time is used. The DC voltage source is obtained by using a three phase diode bridge rectifier and autotransformer. A large CLC filter is used to obtain a ripple free input dc voltage for the inverter. A large electrolytic capacitor (10000 μF) is first used to smoothing the rectifier output voltage. To reduce further the output current ripple of the rectifier, a large filter inductor is used (48 mH). Finally, almost a ripple free dc voltage is obtained by using the second dc filter electrolytic capacitor of 220 μF. During the experiment, the dc voltage was maintained constant at 50 Vdc. The rotor is locked during the experiments so that no emf is generated. Locked rotor conditions are selected because the main purpose of the experiments are verifying the calculated results of inverter input current ripple. Based on measurement results, the resistance and inductance of symmetrical nine-phase motor are 1.84 ohm and 11.44 mH, respectively. Resistance and inductance of asymmetrical nine-phase motor are 2.17 ohm and 10.85 mH, respectively.

Figs. 5 and 6 show inverter output current waveforms for symmetrical and asymmetrical configurations, respectively. Though the switching frequency is not so high, it can be seen that the output current is almost sinusoidal. Figs. 7 and 8 show the inverter output current and input current waveforms for symmetrical and asymmetrical configurations, respectively. These waveforms are captured when the modulation index is unity.

Fig. 9 shows experimental and calculated results of inverter input current ripples under both types of load. During experiments, the fundamental frequency of the inverter output voltage is kept constant at 50 Hz. Validity of the proposed analysis method can be appreciated from this figure. The experimental results have also verified that symmetrical configuration results in less ripple than the asymmetrical one.

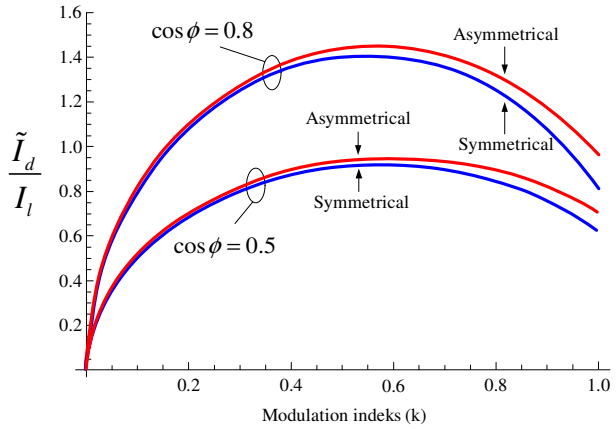

Fig. 3. Input current-ripple under symmetrical and aymmetrical configurations.

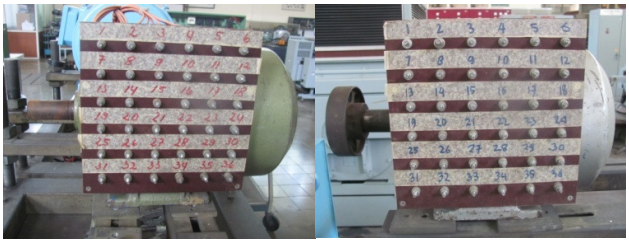

(a) (b)

Fig. 4. Nine-phase motor (a) symmetrical (b) asymmetrical.

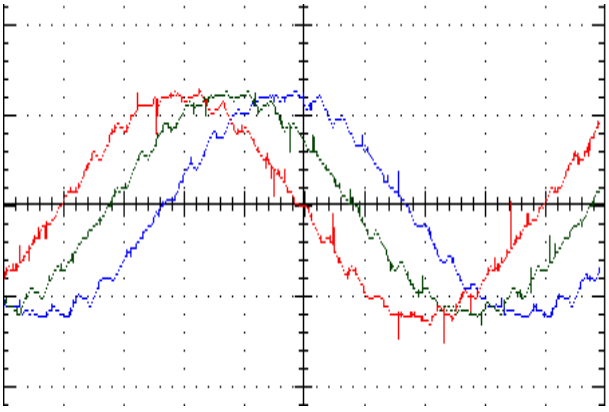

Fig. 5. Output currents i_1, i_2, and i_3 (5 A/div) for symmetrical configuration (2.5 ms/div).

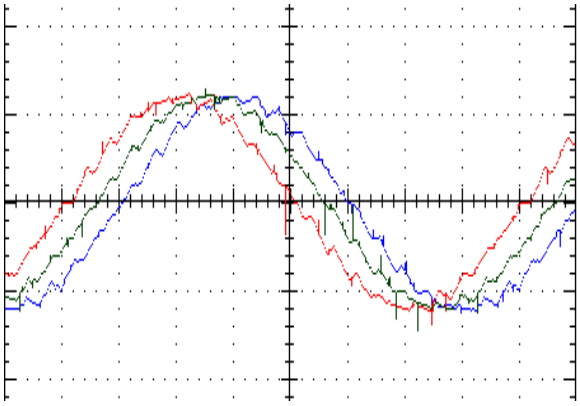

Fig. 6. Output currents i_1, i_2, and i_3 (5 A/div) for asymmetrical configuration (2.5 ms/div).

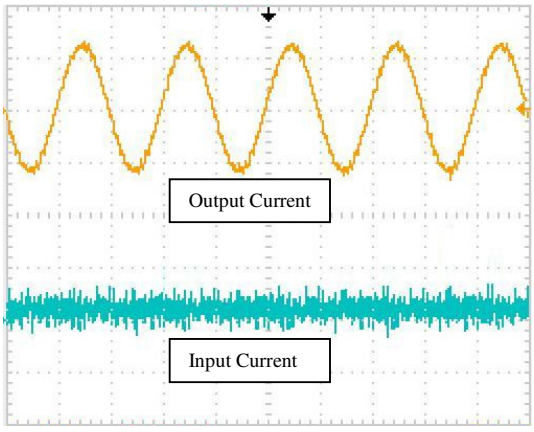

Fig. 7. Output current i_1 (5 A/div) and input current i_d (25 A/div) for symmetrical configuration (10 ms/div).

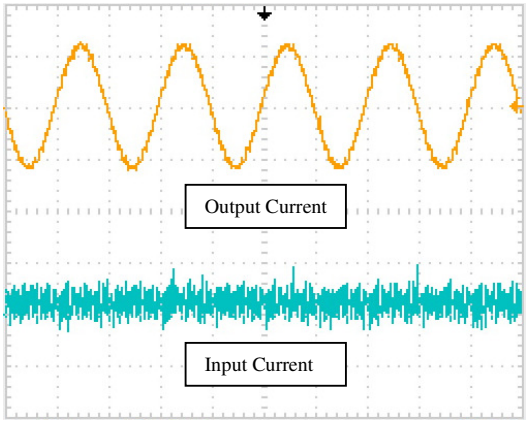

Fig. 8. Output current i_1 (5 A/div) and input current i_d (25 A/div) for asymmetrical configuration (10 ms/div).

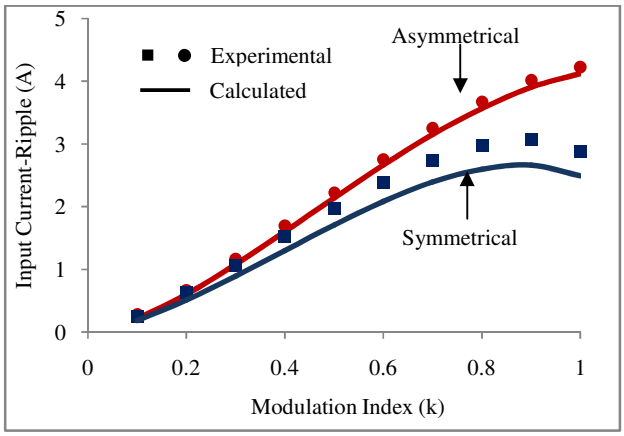

Fig. 9. Experimental and calculated results.

V. Conclusion

Analysis of input current ripple of nine-phase PWM inverter for symmetrical and asymmetrical configurations has been presented in this paper. The rms value of input current ripple of nine-phase PWM inverter is influenced by the output-current, modulation index, and load power-factor. Switching frequency cannot be used to reduce the input current ripple. Symmetrical configuration produces lower input current ripple compared to asymmetrical configuration. Experimental results have verified the validity of the proposed analysis method.

References

[1] E. A. Klingshirn, "High Phase Order Induction Motors," *IEEE Trans. Power App. Sys*., Vol. 102, No. 1, Jan. 1983, pp. 47-59.

[2] C. E. Coates, D. Platt, and V. J. Goesbell, "Performance Evaluation of a Nine-Phase Synchronous Reluctance Drive," *IEEE Ind. Appl. Soc. Ann. Meet*., 2001, pp. 2041-2047.

[3] S. Williamson and S. Smith, "Pulsating Torque and Losses in Multiphase Induction Machines," *IEEE Trans. Ind. Appl*., Vol. 39, No. 4, July/August 2003, pp. 986-993.

[4] E. Levi, "Multiphase Electric Machines for Variable Speed Applications," *IEEE Trans. Ind. Electr*., Vol. 55, No. 5, May 2008, pp. 1893-1908.

[5] A. Tessarolo and C. Bassi, "Stator Harmonic Currents in VS-Fed Synchronous Motors With Multiple Three-Phase Armature Windings," *IEEE Trans. Energy Conv*., Vol. 25, No. 4, Dec. 2010, pp. 974-982.

[6] A. Iqbal, E. Levi, M. Jones, and S. N. Vukosavic, "Generalized Sinusoidal PWM with Harmonic Injection for Multiphase VISs," *IEEE Power Electr. Spec. Conf.*, 2006, pp. 2871-2877.

[7] P. A. Dahono, "Analysis and Minimization of Output Current Ripple of Multiphase PWM Inverters," *IEEE Power Electr. Spec. Conf*., 2006, pp. 3024-2029.

[8] G. Grandi, G. Serra, and A. Tani, "Space Vector Modulation of a Nine-Phase Voltage-Source Inverter," *IEEE Inter. Symp. Ind. Electr.,* 2007, pp. 431-436.

[9] D. Yazdani, S. A. Khajehoddin, A. Bakhshai, and G. Joos, "Fully Utilization of the Inverter in Split-Phase Drives by Means of a Dual Three-Phase Space Vector Classification Algorithm," *IEEE Trans. Ind. Electr*., Vol. 56, No. 1, Jan. 2009, pp. 120-129.

[10] P. D. Ziogas and P. N. D. Photiadis, "An Exact Input Current Analysis of Ideal Static PWM Inverters," *IEEE Trans. Ind. Appl*., Vol. 19, No. 2, March/April 1983, pp. 281-295.

[11] P. A. Dahono, Y. Sato, and T. Kataoka, "Analysis and Minimization of Ripple Components of Input Current and Voltage of PWM Inverters," *IEEE Trans. Ind. Appl*., Vol. 32, No. 4, July/August 1996, pp. 945-950.

[12] J. W. Kolar and S. D. Round, "Analytical Calculation of the RMS Current Stress on the DC Link Capacitor of Voltage-Fed PWM Converter Systems," *IEE Proc. Electr. Power Appl*., Vol. 153, No. 4, July 2006, pp. 535-543.

[13] M. H. Bierhoff and F. W. Fuchs, "DC Link Harmonics of Three-Phase Voltage-Source Converters Influenced by the Pulsewidth Modulation Strategies – An Analysis, *IEEE Trans. Ind. Electr*., Vol. 55, No. 5, May 2008, pp. 2085-2092.

[14] R. Bojoi, M.C. Caponet, G. Grieco, M.Lazzari, A. Tenconi, F. Produmo, "Computation and measurement of the DC link current in six phase volatege source PWM Inverters for AC Motor Drive," *Proc. Power Conv*., Osaka, 2002.

[15] P.A. Dahono, Deni, C. P. Akbarifutra, and A. Rizqiawan, "Input Ripple Analysis of Five-Phase Pulse Width Modulated Inverters," *IET Power Electr*., Vol. 3, No. 5, 2010, pp. 716-723.

[16] B. P. McGrath, D.G. Holmes, " A General Analytical Method for Calculating Inverter DC-Link Current Harmonics", *IEEE Trans Ind. Appl.*, 45, No. 5, Nov/Dec 2009, pp. 1851-1859.